Computer-based analysis of rhegmatogenous retinal detachment

Damiano Natali[1], Rodolfo Repetto[1], Jennifer H. Siggers[2],
Tom H. Williamson[3,4], <u>Jan O. Pralits</u>[1]

[1]Dept of Civil, Chemical and Environmental Engineering, University of Genova, Italy,
[2]Dept of Bioengineering, Imperial College London, London, UK,
[3]Retina Surgery, 50-52 New Cavendish Street, London, UK
[4]NHS, St Thomas Hospital, London, UK

September, 17th 2015

Anatomy of the eye
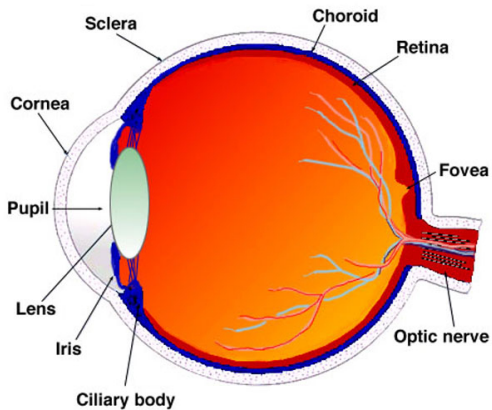
Retinal detachment
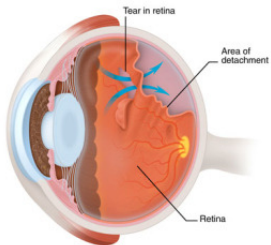
Posterior vitreous detachment (PVD) and vitreous degeneration:

- more common in myopic eyes;
- preceded by changes in vitreous macromolecular structure and in vitreoretinal interface $\rightarrow$ possibly mechanical reasons.
- If the retina detaches from the underlying layers $\rightarrow$ loss of vision;

Rhegmatogeneous retinal detachment:

- fluid enters through a retinal break into the sub retinal space and peels off the retina.

Risk factors:

- **myopia;**
- posterior vitreous detachment (PVD);
- lattice degeneration;
- ...

Scleral buckling and vitrectomy

Scleral bluckling
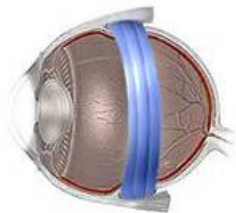
Scleral buckling is the application of a rubber band around the eyeball at the site of a retinal tear in order to promote reachtachment of the retina.

Vitrectomy

The vitreous may be completely replaced with tamponade fluids: silicon oils, water, gas, ..., usually immiscible with the eye's own aqueous humor

The retinal detachment: cases considered here
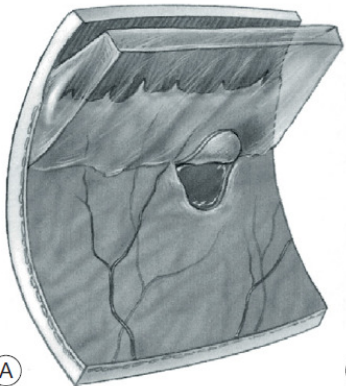
A) horseshoe tear (when large, $>90°$, GRT),   B) retinal hole
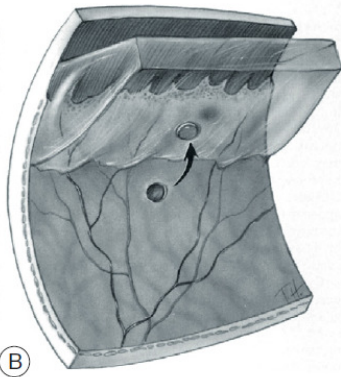
The retinal detachment: cases considered here

Section A-A

Section A-A
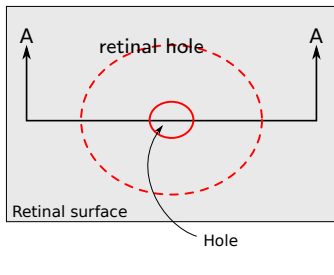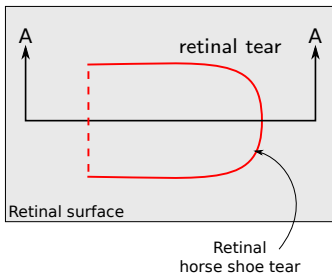
Motivation

Retinal tear and retinal holes are treated using surgery but it is not always clear what type of retinal break and under what conditions is more prone to further detach.

It would therefore be useful to parametrize (size, attachment angles, size of retinal hole, ...) different retinal breaks during eye motion and evaluate a measure of the **tendency to further detach**.
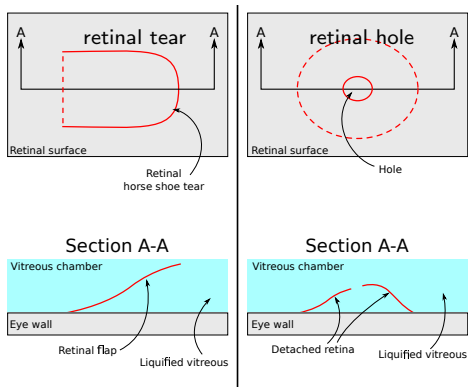
The model - tear configuration
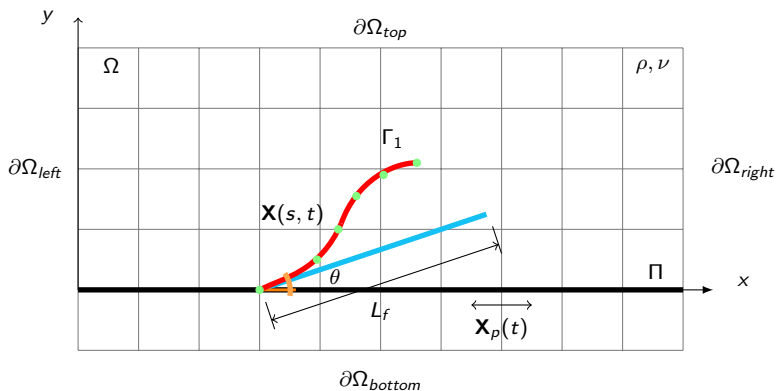
The model - hole configuration
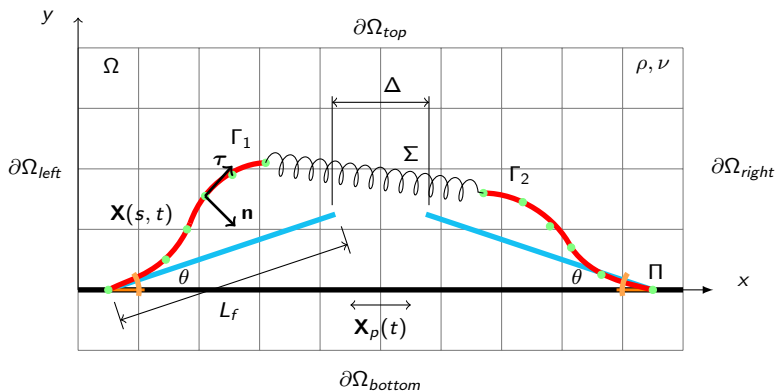
Governing equations
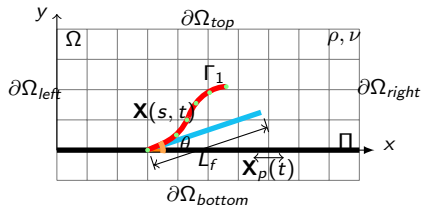
For the viscous incompressible fluid

$$\begin{cases} \dfrac{\partial \mathbf{u}}{\partial t} + \mathbf{u} \cdot \nabla \mathbf{u} = -\nabla p + \dfrac{1}{Re}\nabla^2 \mathbf{u} + \mathbf{f} \\ \nabla \cdot \mathbf{u} = 0 \end{cases} \quad ,$$

Periodicity is imposed at $\partial\Omega_{left}$ and $\partial\Omega_{right}$, and symmetry at $\partial\Omega_{top}$ and $\partial\Omega_{bottom}$. Non slip boundary conditions are imposed on solid surfaces.

For the slender 1D structure

$$\rho_1 \frac{\partial^2 \mathbf{X}}{\partial t^2} = \frac{\partial}{\partial s}\left(T \frac{\partial \mathbf{X}}{\partial s} \right) - \frac{\partial^2}{\partial s^2}\left(K_b \frac{\partial^2 \mathbf{X}}{\partial s^2} \right) + \rho_1 \mathbf{g} - \mathbf{F}$$

The structure is clamped at a certain angle θ at the wall, which moves according to $\mathbf{X_p(t)}$. Incompressibility of the structure is imposed and non-slip/no penetration of the fluid is enforced.

Dimensionless parameters

The governing equations can be non-dimensionalized with the following characteristic scales:

$$x^* = \frac{x}{L}, \mathbf{u}^* = \frac{\mathbf{u}}{U_\infty}, \mathbf{f}^* = \frac{\mathbf{f}L}{\rho_0 U_\infty^2}, \mathbf{F}^* = \frac{\mathbf{F}L}{\rho_1 U_\infty^2}$$

Doing so, several dimensionless parameters arises:

$$Re = \frac{U_\infty L}{\nu}, \quad Fr = \frac{gL}{U_\infty^2}, \quad \rho = \frac{\rho_1}{\rho_0 L}, \quad \gamma = \frac{K_b}{\rho_1 U_\infty^2 L^2}$$

Plate imposed motion

We model isolated rotations using the analytical relationship proposed by Repetto et al. (2005).
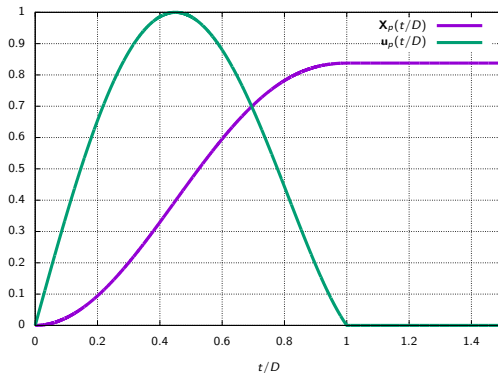
- The angle is 8°
- The maximum velocity is 0.061 m/s
- The duration is 0.045 s

Parameters used in the computations

Quantity	Value	Reference
Properties of the retinal flap		
Density ρ_S	1300 kg/m^3	
Length L	$1.5 - 2.5$ mm	
Thickness	70 μm	Alamouti and Funk (2003), Foster et al. (2010), Ethier et al. (2004), Bowd et al. (2000), Wollensak and Eberhard (2004), Dogramaci and Williamson (2013)
Bending stiffness K_b	$2.98 \cdot 10^{-11}$ Nm^2	$Eh^3/12$
Young's modulus E	$1.21 \cdot 10^3$ N/m2	Jones et al. (1992), Wollensak and Eberhard (2004), Reichenbach et al. (1991), Sigal et al. (2005)
Properties of the fluid		
Density ρ_F	1000 kg/m^3	Foster et al. (2010)
Dynamic viscosity μ	$1.065 \cdot 10^{-3}$ kg/ms	Foster et al. (2010)

Table: Parameter values used for the simulations and corresponding references when available.

Dynamics for retinal tear

L=2 mm, $\theta = 33.6°$

Movie 1

Dynamics for retinal hole

L=2 mm, $\theta = 33.6^\circ$, $\Delta = 0.17$ mm

Movie 2

Clamping force and torque evaluation
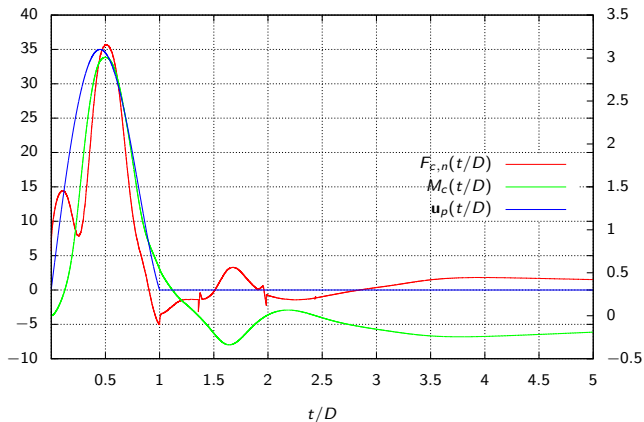
We evaluate the wall-normal force ($F_{c,n}$) and torque (M_c) at the clamping point as a function of time. These values are then used to model the **tendency to further detach**.

Winkler theory
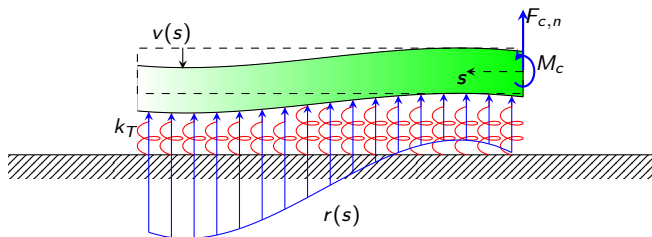
Semi-infinite foundation (in green) subject to a punctual force $F_{c,n}$ and torque M_c at the finite end, and supported by elastic spring of stiffness k_T (in red). The soil reaction $r(s)$ (in blue) is proportional to the foundation displacement $v(s)$.

$$v(s) = \frac{e^{-\alpha s}}{2\alpha^3 \gamma} \{\alpha M_c \left[cos\,(\alpha s) - sin\,(\alpha s) \right] + F_{c,n} cos\,(\alpha s) \},$$

$$d = \max(v|_{s=0}, 0) = \max(\frac{\alpha M_c + F_{c,n}}{2\alpha^3 \gamma}, 0),$$

where α is the ratio between the soil spring rigidity k_T and the foundation beam stiffness γ.

d is the tendency to detach

Tendency to detach
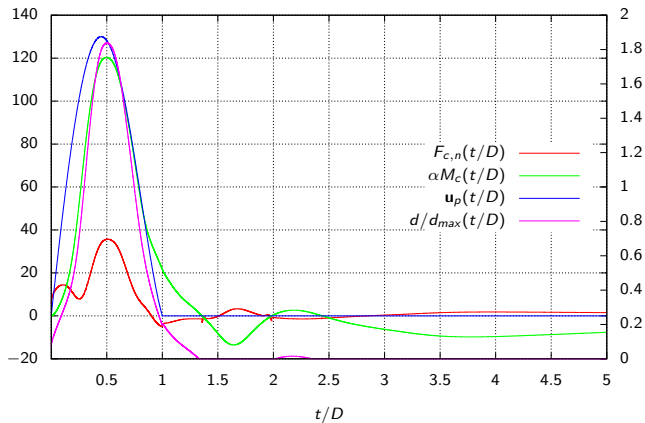
d attains a maximum value for a finite value of t/D

Different filament lengths L: maximum tendency to detach

clamping angle $\theta = 33.56°$, $\Delta = 0.17mm$ (retinal hole)
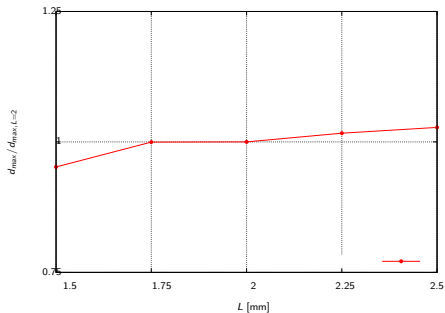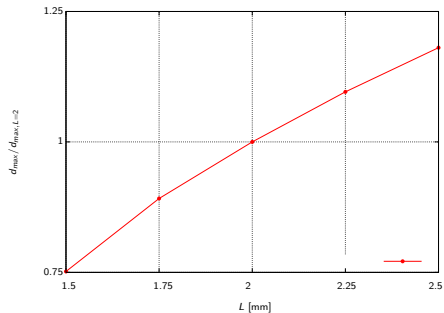
Tear

Hole

Increasing L increases the maximum value of d

Different clamping angles θ: maximum tendency to detach

length $L = 2$ mm, $\Delta = 0.17mm$ (retinal hole)
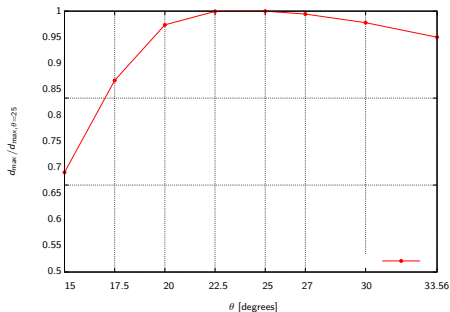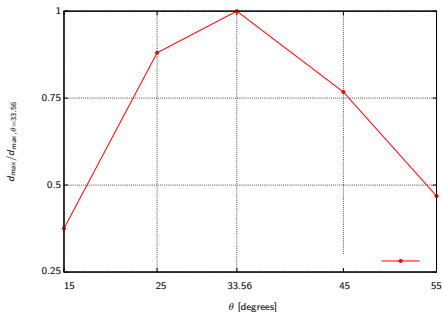
Tear

Hole

A maximum value of d is found

Comparison horseshoe tear & hole: maximum tendency to detach

clamping angle $\theta = 33.56°$, $\Delta = 0.17mm$ (retinal hole)
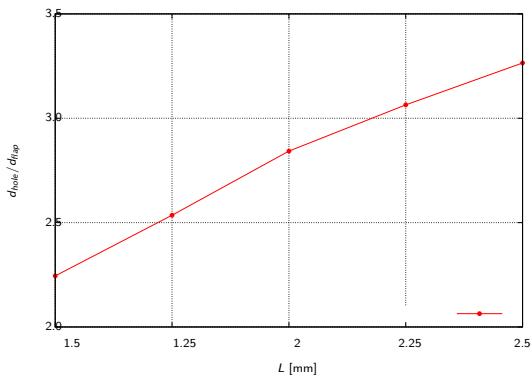
The retinal hole is more prone to detach compared to horseshoe tear

Conclusions

- Numerical investigation of the tendency to further detach two types of retinal breaks (horseshoe tear & hole)

Conclusions

- Numerical investigation of the tendency to further detach two types of retinal breaks (horseshoe tear & hole)
- Achieved solving a fluid-structure interaction problem using a finite-volume code developed in Matlab$^{©}$ with an immersed boundary approach

Conclusions

- Numerical investigation of the tendency to further detach two types of retinal breaks (horseshoe tear & hole)
- Achieved solving a fluid-structure interaction problem using a finite-volume code developed in Matlab$^{©}$ with an immersed boundary approach
- The parameters used are realistic for the human eye (according to the literature)

Conclusions

- Numerical investigation of the tendency to further detach two types of retinal breaks (horseshoe tear & hole)
- Achieved solving a fluid-structure interaction problem using a finite-volume code developed in Matlab$^{©}$ with an immersed boundary approach
- The parameters used are realistic for the human eye (according to the literature)
- The main results show:
  - Increasing the length L increases the tendency to detach (both hole & tear).
  - The maximum tendency to detach is found for a clamping angle of $\approx 25°$ and $\approx 34°$ for tear and hole, respectively.
  - The inter tip distance Δ (hole size) has little effect on the tendency to detach.
  - The tendency to detach of a retinal hole, compared to a tear, is 2 - 3 times larger for retinal filaments of 1.5 - 2.5 mm, with increasing values of d for increasing values of the filament length.

Conclusions

- Numerical investigation of the tendency to further detach two types of retinal breaks (horseshoe tear & hole)
- Achieved solving a fluid-structure interaction problem using a finite-volume code developed in Matlab$^{©}$ with an immersed boundary approach
- The parameters used are realistic for the human eye (according to the literature)
- The main results show:
  - Increasing the length L increases the tendency to detach (both hole & tear).
  - The maximum tendency to detach is found for a clamping angle of $\approx 25°$ and $\approx 34°$ for tear and hole, respectively.
  - The inter tip distance Δ (hole size) has little effect on the tendency to detach.
  - The tendency to detach of a retinal hole, compared to a tear, is 2 - 3 times larger for retinal filaments of 1.5 - 2.5 mm, with increasing values of d for increasing values of the filament length.
- Collaborations with a surgeon confirms that these results will give useful guidelines for treatment of retinal breaks.

References I

B. Alamouti and J. Funk. Retinal thickness decreases with age: an oct study. *British Journal of Ophthalmology*, 87(7):899–901, 2003.

C. Bowd, R. N. Weinreb, B. Lee, A. Emdadi, and L. M. Zangwill. Optic disk topography after medical treatment to reduce intraocular pressure. *American Journal of Ophthalmology*, 130(3): 280 – 286, 2000. ISSN 0002-9394. doi: http://dx.doi.org/10.1016/S0002-9394(00)00488-8. URL http://www.sciencedirect.com/science/article/pii/S0002939400004888.

M. Dogramaci and T. H. Williamson. Dynamics of epiretinal membrane removal off the retinal surface: a computer simulation project. *Br. J. Ophthalmol.*, 97 (9):1202–1207, 2013. doi: 10.1136/bjophthalmol-2013-303598.

C. R. Ethier, M. Johnson, and J. Ruberti. Ocular biomechanics and biotransport. *Annu. Rev. Biomed. Eng.*, 6:249–273, 2004.

W. J. Foster, N. Dowla, S. Y. Joshi, and M. Nikolaou. The fluid mechanics of scleral buckling surgery for the repair of retinal detachment. *Graefe's Archive for Clinical and Experimental Ophthalmology*, 248(1):31–36, 2010.

I. L. Jones, M. Warner, and J. D. Stevens. Mathematical modelling of the elastic properties of retina: a determination of young's modulus. *Eye*, (6):556–559, 1992.

A. Reichenbach, W. Eberhardt, R. Scheibe, C. Deich, B. Seifert, W. Reichelt, K. Dähnert, and M. Rödenbeck. Development of the rabbit retina. iv. tissue tensility and elasticity in dependence on topographic specializations. *Experimental Eye Research*, 53(2):241 – 251, 1991. ISSN 0014-4835. doi: http://dx.doi.org/10.1016/0014-4835(91)90080-X. URL http://www.sciencedirect.com/science/article/pii/001448359190080X.

References II

R. Repetto, A. Stocchino, and C. Cafferata. Experimental investigation of vitreous humour motion within a human eye model. *Phys. Med. Biol.*, 50:4729–4743, 2005.

I. A. Sigal, J. G. Flanagan, and C. R. Ethier. Factors influencing optic nerve head biomechanics. *Investigative Ophthalmology & Visual Science*, 46(11):4189, 2005. doi: 10.1167/iovs.05-0541. URL +http://dx.doi.org/10.1167/iovs.05-0541.

G. Wollensak and S. Eberhard. Biomechanical characteristics of retina. *Retina*, (24):967–970, 2004.